

\mathcal{H}_∞ Stabilization of the Current Profile in Tokamak Plasmas via LMI Approach [★]

Oumar Gaye ^{a,d}, Laurent Autrique ^a, Yury Orlov ^b, Emmanuel Moulay ^c,
Sylvain Brémond ^d, Rémy Nouailletas ^d

^a Université d'Angers, 62 avenue Notre Dame du Lac, 49000 Angers – France

^b CICESE Research Center, Km. 107, Carretera Tijuana-Ensenada, B.C. 22 860 – Mexico

^c Xlim-SIC (UMR CNRS 6172), Université de Poitiers, 86962 Futuroscope Chasseneuil Cedex – France

^d CEA/DSM/IRFM CEA-Cadarache, 13108 Saint Paul Lez Durance – France

Abstract

This paper deals with the \mathcal{H}_∞ stabilization of the spatial distribution of the current profile of tokamak plasmas using a Linear Matrix Inequalities (LMIs) approach. The control design is based on the one dimensional resistive diffusion equation of the magnetic flux that governs the plasma current profile evolution. The feedback control law is derived in the infinite dimensional setting without spatial discretisation. The proposed distributed control is based on a proportional-integral state feedback taking into account both interior and boundary engineering actuators. Supporting numerical simulations are presented and tuning of the controller parameters attenuating uncertain disturbances is discussed.

Key words: Tokamak plasmas control; Parabolic partial differential equations; Lyapunov stabilization; \mathcal{H}_∞ control; LMI.

1 Introduction

Considering polluting effects, fossil fuel energy cannot be a source of energy capable of satisfying the requirements of industry developments and the needs of the increasing world population. In such a context, nuclear fusion is an attractive alternative since fusion produces neither air pollution nor greenhouse gases: during the reaction two light nuclei (deuterium and tritium) are stuck together to form a heavier nucleus (helium) plus an energetic neutron. Moreover, both elements (deuterium and tritium) are wide spread over the world: deuterium can be extracted from sea water, while lithium, that has to be used to breed tritium, can be found in continental crust. The key goal of the world project ITER (led by

seven partners: EU, U S A, Japan, China, India, South Korea, Russia) is to demonstrate the scientific feasibility of thermonuclear fusion [32]. The fusion reaction requires extremely high temperatures ($> 50 \cdot 10^6$ Kelvin) for which hydrogen gas, in the plasma state, has to be confined. One of the most used configuration is the so-called torus-like tokamak [29]. Magnetic field (toroidal and poloidal) confinement is obtained by superimposing various electric currents, including a high current, of the MegaAmpere range, within the plasma itself. This plasma current can be produced by non-inductive means through the injection of fast particles and/or waves and by inductive means, in particular at the beginning of the plasma pulses. The 1D radial profile of this plasma current is a key plasma parameter. It plays a crucial role in the global magnetohydrodynamic (MHD) stability of plasma experiments [29] and it has also been observed that some specific profiles may generate enhanced confinement of the plasma energy (internal transport barrier). The current density profile depends on the spatial derivative of the poloidal flux, whose dynamics is governed by the so-called resistive diffusion of the poloidal flux.

[★] Corresponding author Laurent Autrique. Tel. +33 (0)2 41 22 65 00. Fax +33 (0) 241 226 518.

Email addresses: oumar.gaye@etud.univ-angers.fr (Oumar Gaye), laurent.autrique@univ-angers.fr (Laurent Autrique), yorlov@cicese.mx (Yury Orlov), emmanuel.moulay@univ-poitiers.fr (Emmanuel Moulay), sylvain.bremond@cea.fr (Sylvain Brémond), remy.nouailletas@cea.fr (Rémy Nouailletas).

The control of internal plasma radial profiles is still in its infancy, although several studies have been performed on experimental devices like Tore Supra (France), DIII-D (USA), JET (Joint European Torus, UK), or JT-60U (Japan Torus). The closed-loop control of one single shape parameter, based on Single Input - Single Output (SISO) semi-empirical modelling, has been experimentally achieved (e.g control of plasma internal inductance [30] or non-inductive current drive profile width [3]). More recently, stationary states of the safety factor profile, defined by their MHD activity, were feedback controlled on Tore Supra [17]. However this is clearly not enough to match the main requirements of MHD stability and/or internal transport barriers issues [10]. The control of the safety factor profile in a few number of points, based on a Multi Input Multi Output (MIMO) approach in finite dimensional setting was developed using linear models identified from experimental data [21]. The control of coupled magnetic (safety factor) and kinetic (pressure) profiles was experimentally tested in particular on the Joint European Torus (JET) tokamak [20] but showed severe limitations in terms of sensitivity to the operating conditions, given also the lack of power from the actuators. In [33], a proper orthogonal decomposition is proposed in order to consider a low dimensional dynamical system. Then by using model reduction, optimal feedback control of the nonlinear parabolic partial differential equations (PDEs) is connected to iterative optimal control methodologies for finite dimensional systems. Some other recent approaches have been developed on simulations, [7,8,14,25,26].

In the present work a new approach is proposed for the control of the investigated parabolic system with boundary and interior actuation mechanism. The feedback control law is defined in the infinite dimensional setting without spatial discretization. For this purpose, \mathcal{H}_∞ control is developed within the framework of linear matrix inequality (LMI) approach [6], recently extended in [13] to the PDE setting. Numerical simulations are performed based on the Tore Supra tokamak plant. In fact, this experimental device is the real engineering plant. The Tore Supra tokamak is highly relevant in terms of time scales: most of the previous work targeted tokamak facilities where steady state of plasma internal profiles, especially plasma safety factor/current profile is hardly achievable, at least at the plasma center. With its capability to run long lasting plasma discharge up to several minutes (Tore Supra has made a more than 6 minutes long 1 GJ world record plasma discharge), and to drive large non inductive current (about 500 kA of lower hybrid current have already been driven during more than one minute long discharges, and the current drive capabilities will be further increased with the completion of the on-going lower hybrid system upgrade), the Tore Supra tokamak offers an unique opportunity to develop and test plasma safety factor / current profile control schemes on relevant time scales.

The primary concern of the paper is to synthesize proportional and proportional integral \mathcal{H}_∞ regulators of tokamak internal plasma profiles in the PDE's setting. A target profile, that should constitute the steady-state of the closed-loop system, is designed *a priori*, using manipulatable inputs of the system such as the loop voltage, the lower hybrid power, and the wave refractive index. It is worth noticing that while being of a parabolic type, the underlying PDE is not, however, typical in the control of distributed parameter systems as it contains a non self-adjoint infinitesimal operator (the principal higher order differential term) in the state equation. To the best of our knowledge, controlling such a kind of PDE's has not been developed so far and presenting *an LMI-based framework for the distributed \mathcal{H}_∞ control of such a plant is a clear contribution* the paper makes into the existing literature. Once a spatially distributed \mathcal{H}_∞ regulator is designed, it is on-line optimally approximated by the best set of real engineering inputs (the loop voltage, the lower hybrid power, and the wave refractive index) which are then applied to the plant. Since it is hardly possible to involve the shape constraints on the engineering inputs into the \mathcal{H}_∞ design, these constraints are brought into play while approximating the constructed \mathcal{H}_∞ regulator via the constrained optimization procedure. Although the proposed approach to the current profile regulation in tokamak plasmas is developed *ad hoc* it is then supported by the numerical study made with the tokamak plant simulator METIS (Minute Embedded Tokamak Integrated Simulator) [2].

The paper is organized as follows. In section 2, the mathematical model is presented. The model is based on the 1D resistive diffusion PDE of the magnetic flux that governs the plasma current profile evolution. In section 3, a basic distributed proportional controller is exposed and exponential stabilization is proved. Section 4 is devoted to the design of a distributed proportional and integral controller. For both control laws, theoretical developments are proposed in order to prove the \mathcal{H}_∞ controller efficiency in spite of external disturbances. Finally, simulation results (using the METIS code dedicated to plasma scenario studies) are presented in section 5 and concluding remarks are collected in section 6.

2 Modeling and problem statement

Provided usual assumptions (axisymetry, MHD equilibrium, averaging over the magnetic surfaces, cylindrical approximation, etc. see [5,31] and Fig. 1), the evolution of the plasma current profile q , being the safety factor to be controlled, can be obtained by solving the following 1D PDE

$$\begin{cases} \frac{\partial \psi}{\partial t}(t, x) = \frac{\eta_{||}(t, x)}{\mu_0 a^2} \frac{1}{x} \frac{\partial}{\partial x} \left(x \frac{\partial \psi}{\partial x}(t, x) \right) \\ \quad + \eta_{||}(t, x) R_0 j_{ni}(t, x); \\ \frac{\partial \psi}{\partial x}(t, x) \Big|_{x=0} = 0, \quad \frac{\partial \psi}{\partial t}(t, 1) = -V_0(t). \end{cases} \quad (1)$$

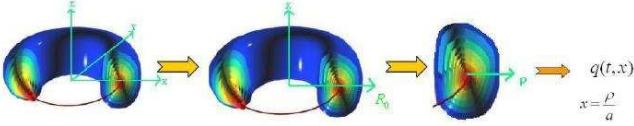


Fig. 1. 1D geometry simplified formulation

and determining it according to

$$q(t, x) = -\frac{a^2 x B_0}{\frac{\partial \psi}{\partial x}(t, x)}. \quad (2)$$

In the above relations, $x \in [0, 1]$ is the 1D (radial) profile coordinate, t the time, $\psi(t, x)$ the magnetic flux, R_0 and a are respectively the major and minor radius of the plasma boundary (both R_0 and a are controlled with high accuracy to be constant [22]), $\mu_0 > 0$ the permeability of vacuum, $\eta_{||}(t, x)$ the parallel electrical resistivity of the plasma, $V_0(t)$ the plasma loop voltage, B_0 the toroidal magnetic field at R_0 , and $j_{ni}(t, x)$ the non-inductive current density. It is of interest to note that the total current density $j_T(t, x)$ is given by

$$j_T(t, x) = -\frac{1}{\mu_0 R_0 a^2 x} \frac{\partial}{\partial x} \left(x \frac{\partial \psi}{\partial x}(t, x) \right) \quad (3)$$

and it allows one to represent the principal term $\frac{\eta_{||}(t, x)}{\mu_0 a^2} \frac{1}{x} \frac{\partial}{\partial x} \left(x \frac{\partial \psi}{\partial x}(t, x) \right)$ in the right hand side of the PDE (1) in the form $-\eta_{||}(t, x) R_0 j_T(t, x)$, similar to that of the additive term $\eta_{||}(t, x) R_0 j_{ni}(t, x)$ in the same. Adequacy of (1) with physically investigated phenomena as well as the solution existence and uniqueness are argued in [9].

Our control objective is to track a desired safety factor profile which does not depend directly on ψ but which depends on its spatial derivative $\frac{\partial \psi}{\partial x}$.

In order to deal with homogeneous boundary conditions, let us introduce the following state transformation

$$\psi_r(t, x) = \psi(t, x) - \psi(t, 1). \quad (4)$$

Taking into account (2), we have

$$\psi_r(t, x) = a^2 B_0 \int_x^1 \frac{r}{q(t, r)} dr.$$

The control variables in the infinite dimensional setting are the plasma loop voltage $V_0(t)$ and the non-inductive current density $j_{ni}(t, x)$. $V_0(t)$ can basically directly be set using the inner poloidal magnetic field coils voltage whereas $j_{ni}(t, x)$ is manipulated indirectly, using the lower hybrid power P_{lh} and the wave refractive index

N_{lh} . The state equation (1), rewritten in terms of ψ_r , reduces to

$$\begin{cases} \frac{\partial \psi_r}{\partial t}(t, x) = \frac{\eta_{||}(t, x)}{\mu_0 a^2} \frac{1}{x} \frac{\partial}{\partial x} \left(x \frac{\partial \psi_r}{\partial x}(t, x) \right) \\ \quad + \eta_{||}(t, x) R_0 j_{ni}(t, x) + V_0(t), \\ \frac{\partial \psi_r}{\partial x}(t, x) \Big|_{x=0} = 0, \quad \psi_r(t, 1) = 0 \end{cases} \quad (5)$$

Then, let us introduce the error variable

$$\phi(t, x) = \psi_r(t, x) - \psi_r^{target}(x) \quad (6)$$

with respect to a target $\psi_r^{target}(x)$ which we intend to reach in the inner-product space

$$\mathbf{W} = \{ \Psi \in \mathbf{H}^2(0, 1) : \frac{\partial \Psi}{\partial x} \Big|_{x=0} = \Psi(1) = 0 \} \quad (7)$$

of differentiable functions equipped with the inner product $\langle \Psi_1, \Psi_2 \rangle_{L_2(0,1)} = \int_0^1 \Psi_1(x) \Psi_2(x) x dx$, inducing the norm $\| \Psi \|_{L_2(0,1)} = \sqrt{\int_0^1 |\Psi(x)|^2 x dx}$ (for more information about weighted L_2 spaces see [19]). As a matter of fact, the target $\psi_r^{target}(x)$, designed *a priori*, using the manipulatable inputs V_0 and $j_{ni} = j_{ni}(P_{lh}, N_{lh})$, should meet the same homogeneous boundary conditions

$$\frac{\partial \psi_r^{target}}{\partial x}(x) \Big|_{x=0} = 0, \quad \psi_r^{target}(1) = 0 \quad (8)$$

as those in (5). The error variable is then governed by

$$\begin{cases} \frac{\partial \phi}{\partial t}(t, x) = \frac{\eta_{||}(t, x)}{\mu_0 a^2} \frac{1}{x} \frac{\partial}{\partial x} \left(x \frac{\partial \phi}{\partial x}(t, x) \right) \\ \quad + \frac{\eta_{||}(t, x)}{\mu_0 a^2} \frac{1}{x} \frac{\partial}{\partial x} \left(x \frac{\partial \psi_r^{target}}{\partial x}(x) \right) \\ \quad + \eta_{||}(t, x) R_0 j_{ni}(t, x) + V_0(t); \\ \frac{\partial \phi}{\partial x}(t, x) \Big|_{x=0} = 0, \quad \phi(t, 1) = 0. \end{cases} \quad (9)$$

In order to deal with the regular additive terms in the right hand side of the PDE (9) we assume that

$$\frac{1}{x} \frac{\partial}{\partial x} \left(x \frac{\partial \psi_r^{target}}{\partial x}(x) \right) \in \mathbf{W}. \quad (10)$$

Let us now introduce the following term

$$\eta_{||}(t, x) R_0 j_{control} = \eta_{||}(t, x) R_0 j_{ni}(t, x) + V_0(t) \quad (11)$$

in order to subsequently synthesize a stabilizing control law. The non-inductive current density $j_{ni}(t, x)$ is composed of the bootstrap current density $j_{bs}(t, x)$ (which is self-generated by the plasma, [16]) and of additional source terms provided by different actuators, namely the Lower Hybrid, Electron Cyclotron or Ion Cyclotron

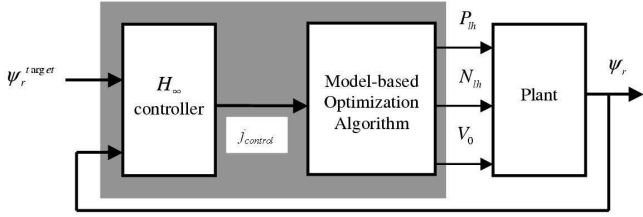


Fig. 2. Control scheme of the system

wave systems and/or the Neutral Beam Injection system. The most efficient is the Lower Hybrid Current Drive (LHCD) system that is routinely used on the Tore Supra Tokamak [27], which now has a capability to inject up to around 7 MW in steady state that will allow to sustain plasma currents in the MegaAmpere range on very long pulse [4]. The distributed control law design (proportional and proportional-integral) is generic to all kinds of current drive system. However, in this paper, the numerical simulations will be performed on Tore Supra typical conditions, using mainly Lower Hybrid waves as current drive means, so that in this particular case

$$j_{ni}(t, x) = j_{bs}(t, x) + j_{lh}(t, x) \quad (12)$$

where $j_{bs}(t, x)$ and $j_{lh}(t, x)$ are respectively the bootstrap current density and the current density provided by the LHCD system. The unactuated variable $j_{bs}(t, x)$ can be modelled by a nonlinear function of the flux and pressure [16] and thus can be estimated on-line, but it cannot be varied according to the control demand. In turn, $j_{lh}(t, x)$ is modelled by Gaussian functions which are controlled by two engineering parameters, the LH power P_{lh} and the wave refractive index N_{lh} (see [31] for further details). In the simulations of section 5, the variables V_0 , P_{lh} and N_{lh} are viewed as the time-varying control inputs whereas $j_{bs}(t, x)$ as an external disturbance to be attenuated/compensated.

In the present investigation, the resistivity $\eta_{||}(t, x)$ is assumed to be lower and upper bounded by some positive constants η_1 and η_2 , i.e.

$$\eta_1 \leq \eta_{||}(t, x) \leq \eta_2 \quad (13)$$

for all $x \in [0, 1]$ and $t \geq 0$. Apart from this, we assume that $\eta_{||}(t, x)$ is differentiable in t for all $x \in [0, 1]$ and by taking into account that $\eta_{||}(t, x)$ depends on the temperature of the plasma, whose time rate of change is rather slow, we also assume that the time derivative of $\eta_{||}(t, x)$ is uniformly bounded

$$\left| \frac{\partial \eta_{||}(t, x)}{\partial t} \right| < \Delta \quad (14)$$

by some constant $\Delta > 0$. Moreover, we consider that $\eta_{||}(t, x)$ is available for feedback purposes through some

on-line estimation, basically from electronic temperature measurements (see [31] for more details). The feedback control strategy adopted in this paper is composed of two steps shown in Fig. 2. The first step is to synthesize the current density $j_{control}$ to be applied to the system. The resulting \mathcal{H}_∞ controller is designed in the infinite dimensional setting where a target flux profile ψ_r^{target} and current flux profile serve as inputs. The second step consists of an optimization process which finds the best set of engineering inputs $P_{lh}(t)$, $N_{lh}(t)$ and $V_0(t)$ to fit (as fine as possible) the desired current density control $j_{control}$ generated by the \mathcal{H}_∞ control law in the infinite dimensional setting. The optimization algorithm has to minimize the criterion

$$\varepsilon = \int_0^1 (j_{control} - j_{engineering}(P_{lh}, N_{lh}, V_0))^2 dx \quad (15)$$

under the constraints: $V_{\min} < V_0 < V_{\max}$, $P_{\min} < P_{lh} < P_{\max}$ and $N_{\min} < N_{lh} < N_{\max}$. $j_{engineering}$ is the control profile that can actually be generated with the real plant control variables P_{lh} , N_{lh} and V_0 [26]. In simulations presented in section 5, minimum/maximum value of engineering inputs are taken from the Tore Supra Tokamak constraints, i.e., $-5V < V_0 < 5V$, $0MW < P_{lh} < 7MW$ and $1.43 < N_{lh} < 2.37$. In following sections two distributed controllers are presented.

3 Proportional state feedback synthesis

The main goal of this section is to show that our system is exponentially stabilizable using a proportional feedback. The controller specification (11) simplifies (9) to the PDE

$$\begin{cases} \frac{\partial \phi}{\partial t}(t, x) = \frac{\eta_{||}(t, x)}{\mu_0 a^2} \frac{1}{x} \frac{\partial}{\partial x} \left(x \frac{\partial \phi}{\partial x}(t, x) \right) \\ \quad + \frac{\eta_{||}(t, x)}{\mu_0 a^2} \frac{1}{x} \frac{\partial}{\partial x} \left(x \frac{\partial \psi_r^{target}}{\partial x}(x) \right) \\ \quad + \eta_{||}(t, x) R_0 j_{control} \\ \frac{\partial \phi}{\partial x}(t, x) \Big|_{x=0} = 0, \quad \phi(t, 1) = 0 \end{cases} \quad (16)$$

with homogeneous boundary conditions. The control objective is to synthesize $j_{control}$ such that the error state ϕ is exponentially stable.

3.1 Disturbance-free stabilization

The control problem of partial differential equations (PDEs) is an active area of research [11,18,23,28], but very few constructive methods are available. For robust stabilization, the \mathcal{H}_∞ controller is proposed. We consider the following feedback strategy

$$\begin{aligned} \eta_{||}(t, x) R_0 j_{control} = & -k\phi(t, x) \\ & - \frac{\eta_{||}(t, x)}{\mu_0 a^2} \frac{1}{x} \frac{\partial}{\partial x} \left(x \frac{\partial \psi_r^{target}}{\partial x}(x) \right). \end{aligned} \quad (17)$$

Then the closed-loop system (16), driven by (17), takes the form

$$\begin{cases} \frac{\partial \phi}{\partial t}(t, x) = \frac{\eta_{||}(t, x)}{\mu_0 a^2} \frac{1}{x} \frac{\partial}{\partial x} \left(x \frac{\partial \phi}{\partial x}(t, x) \right) - k \phi(t, x); \\ \left. \frac{\partial \phi}{\partial x}(t, x) \right|_{x=0} = 0, \quad \phi(t, 1) = 0. \end{cases} \quad (18)$$

In the following, the proposed controller (17) is analyzed in order to prove the exponential stability of (18). For later use, we need a technical lemma (Poincaré type inequalities).

Lemma 1 *Let $L(\cdot) \in \mathbf{W}$ and let $w(\cdot)$ be a Lebesgue-measurable function on $[0, 1]$ such that the relations $w_1 \leq w(x) \leq w_2$ are satisfied for all $x \in [0, 1]$ and some positive constants w_1, w_2 . Then the inequality*

$$\int_0^1 |L(x)|^2 \frac{x}{w(x)} dx \leq K \int_0^1 \left| \frac{\partial L(x)}{\partial x} \right|^2 \frac{x}{w(x)} dx \quad (19)$$

holds true with the positive constant $K = \frac{w_2}{ew_1}$.

Proof It is clear that

$$L(1) - L(x) = \int_x^1 \frac{\partial L(s)}{\partial s} ds. \quad (20)$$

Since $L \in \mathbf{W}$ it follows from (7) that $L(1) = 0$ and hence

$$-L(x) = \int_x^1 \frac{\partial L(s)}{\partial s} ds. \quad (21)$$

Then one derives that

$$\begin{aligned} |L(x)|^2 &= \left| \int_x^1 \sqrt{\frac{s}{w(s)}} \frac{\partial L(s)}{\partial s} \frac{\sqrt{w(s)}}{\sqrt{s}} ds \right|^2 \\ &\leq \left(\int_x^1 \left| \frac{\partial L(s)}{\partial s} \right|^2 \frac{s}{w(s)} ds \right) \int_x^1 \frac{w(s)}{s} ds \\ &\leq \left(\int_x^1 \left| \frac{\partial L(s)}{\partial s} \right|^2 \frac{s}{w(s)} ds \right) w_2 (\ln(1) - \ln x) \\ &\leq \left(\int_x^1 \left| \frac{\partial L(s)}{\partial s} \right|^2 \frac{s}{w(s)} ds \right) w_2 (-\ln x). \end{aligned} \quad (22)$$

So, it leads to

$$\begin{aligned} \frac{x}{w(x)} |L(x)|^2 &\leq \left(\int_x^1 \left| \frac{\partial L(s)}{\partial s} \right|^2 \frac{s}{w(s)} ds \right) \frac{w_2}{w(x)} (-x \ln x) \\ &\leq \left(\int_x^1 \left| \frac{\partial L(s)}{\partial s} \right|^2 \frac{s}{w(s)} ds \right) \frac{w_2}{w_1} (-x \ln x) \\ &\leq K \int_x^1 \left| \frac{\partial L(s)}{\partial s} \right|^2 \frac{s}{w(s)} ds \end{aligned} \quad (23)$$

with $K = \frac{w_2}{w_1} \sup_{x \in (0,1)} \{-x \ln x\} = \frac{w_2}{w_1 e}$. Thus the required inequality (19) is established. \square

Theorem 1 *Consider the error system (16) with the above assumptions and let (16) be driven by controller (17). Then the closed-loop system (18) is globally exponentially stable with respect to the induced norm $\|\cdot\|_{L_2(0,1)}$ provided that the controller gain k is tuned according to*

$$k > -\frac{\eta_1^2 e}{\mu_0 a^2 \eta_2} + \frac{\Delta}{2\eta_1}. \quad (24)$$

Proof Consider the following time-varying functional

$$V(\phi(t, \cdot), t) = \int_0^1 \phi(t, x)^2 \frac{x}{\eta_{||}(t, x)} dx \quad (25)$$

which is positive definite and radially unbounded

$$\eta_2^{-1} \|\phi\|_{L_2(0,1)}^2 \leq V(\phi(t, \cdot), t) \leq \eta_1^{-1} \|\phi\|_{L_2(0,1)}^2 \quad (26)$$

where η_1 and η_2 are the lower and upper bounds in (13). The time derivative of (25) is given by

$$\begin{aligned} \frac{dV(\phi(t, \cdot), t)}{dt} &= \int_0^1 \frac{\partial}{\partial t} \left(\phi(t, x)^2 \frac{x}{\eta_{||}(t, x)} \right) dx \\ &= 2 \int_0^1 \frac{\partial \phi(t, x)}{\partial t} \phi(t, x) \frac{x}{\eta_{||}(t, x)} dx \\ &\quad - \int_0^1 \phi(t, x)^2 \frac{x}{\eta_{||}(t, x)} \frac{\partial \eta_{||}(t, x)}{\partial t} dx. \end{aligned} \quad (27)$$

While being computed along the solutions of (18), the time derivative (27) integrates by parts to

$$\begin{aligned} \frac{dV(\phi(t, \cdot), t)}{dt} &= 2 \int_0^1 \frac{\partial \phi(t, x)}{\partial t} \phi(t, x) \frac{x}{\eta_{||}(t, x)} dx \\ &\quad - \int_0^1 \phi(t, x)^2 \frac{x}{\eta_{||}(t, x)} \frac{\partial \eta_{||}(t, x)}{\partial t} dx \\ &= -2k \int_0^1 \phi(t, x)^2 \frac{x}{\eta_{||}(t, x)} dx \\ &\quad + \frac{2}{\mu_0 a^2} \int_0^1 \frac{\partial}{\partial x} \left(x \frac{\partial \phi(t, x)}{\partial x} \right) \phi(t, x) dx \\ &\quad - \int_0^1 \phi(t, x)^2 \frac{x}{\eta_{||}(t, x)} \frac{\partial \eta_{||}(t, x)}{\partial t} dx \\ &= -2k \int_0^1 \phi(t, x)^2 \frac{x}{\eta_{||}(t, x)} dx \\ &\quad - \frac{2}{\mu_0 a^2} \int_0^1 \left| \frac{\partial \phi(t, x)}{\partial x} \right|^2 x dx \\ &\quad - \int_0^1 \phi(t, x)^2 \frac{x}{\eta_{||}(t, x)} \frac{\partial \eta_{||}(t, x)}{\partial t} dx \end{aligned} \quad (28)$$

thereby yielding

$$\begin{aligned} \frac{dV(\phi(t, \cdot), t)}{dt} &= -2k \int_0^1 \phi(t, x)^2 \frac{x}{\eta_{||}(t, x)} dx \\ &\quad - \frac{2}{\mu_0 a^2} \int_0^1 \eta_{||}(t, x) \left| \frac{\partial \phi(t, x)}{\partial x} \right|^2 \frac{x}{\eta_{||}(t, x)} dx \\ &\quad - \int_0^1 \phi(t, x)^2 \frac{x}{\eta_{||}(t, x)} \frac{\partial \eta_{||}(t, x)}{\partial t} dx \\ &\leq -2k \int_0^1 \phi(t, x)^2 \frac{x}{\eta_{||}(t, x)} dx \\ &\quad - \frac{2\eta_1}{\mu_0 a^2} \int_0^1 \left| \frac{\partial \phi(t, x)}{\partial x} \right|^2 \frac{x}{\eta_{||}(t, x)} dx \\ &\quad - \int_0^1 \phi(t, x)^2 \frac{x}{\eta_{||}(t, x)} \frac{\partial \eta_{||}(t, x)}{\partial t} dx. \end{aligned} \quad (29)$$

Specifying inequality (19) with $w(\cdot) = \eta_{||}(t, x)$ and $L(\cdot) = \phi(t, x)$ ($K = \frac{\eta_2}{\eta_1 e}$), the resulting inequality

$$\int_0^1 |\phi(t, x)|^2 \frac{x}{\eta_{||}(t, x)} dx \leq K \int_0^1 \left| \frac{\partial \phi(t, x)}{\partial x} \right|^2 \frac{x}{\eta_{||}(t, x)} dx \quad (30)$$

allows one to conclude from (29) that

$$\begin{aligned} \frac{1}{2} \frac{dV(\phi(t, \cdot), t)}{dt} &\leq - \left(\frac{\eta_1^2 e}{\mu_0 a^2 \eta_2} + k \right) \int_0^1 \phi(t, x)^2 \frac{x}{\eta_{||}(t, x)} dx \\ &\quad + \frac{1}{2} \int_0^1 \phi(t, x)^2 \frac{x}{\eta_{||}(t, x)} \left| \frac{\partial \eta_{||}(t, x)}{\partial t} \right| dx. \end{aligned} \quad (31)$$

Taking (14) into account, it follows

$$\begin{aligned} \frac{1}{2} \frac{dV(\phi(t, \cdot), t)}{dt} &\leq - \left(\frac{\eta_1^2 e}{\mu_0 a^2 \eta_2} + k - \frac{\Delta}{2\eta_1} \right) \int_0^1 \phi(t, x)^2 \frac{x}{\eta_{||}(t, x)} dx \\ &= - \left(\frac{\eta_1^2 e}{\mu_0 a^2 \eta_2} + k - \frac{\Delta}{2\eta_1} \right) V(\phi(t, \cdot), t). \end{aligned} \quad (32)$$

Then

$$V(\phi(t, \cdot), t) \leq V(\phi(0, \cdot), 0) e^{-2ct} \quad (33)$$

with $c = \left(\frac{\eta_1^2 e}{\mu_0 a^2 \eta_2} + k - \frac{\Delta}{2\eta_1} \right) > 0$ due to (24). By virtue of (26), the global exponential stability of the closed-loop system (18) is then concluded in the state space \mathbf{W} . \square

3.2 Disturbance attenuation

The goal of this subsection is to show that the controller defined by (17) solves an \mathcal{H}_∞ control problem with a disturbance attenuation γ (see [12]). Let us consider some perturbations occurring on system (18)

$$\begin{cases} \frac{\partial \phi}{\partial t}(t, x) = \frac{\eta_{||}(t, x)}{\mu_0 a^2} \frac{1}{x} \frac{\partial}{\partial x} \left(x \frac{\partial \phi}{\partial x}(t, x) \right) - k \phi(t, x) \\ \quad + h(t, x) \\ \frac{\partial \phi}{\partial x}(t, x) \Big|_{x=0} = 0, \quad \phi(t, 1) = 0 \end{cases} \quad (34)$$

where $h \in L_2(0, \infty; \mathbf{W})$ is the external disturbance, $L_2(0, \infty; \mathbf{W})$ is the Hilbert space of square integrable Hilbert space-valued functions $h(\cdot, x) \in L_2(0, \infty)$ with values $h(t, \cdot) \in \mathbf{W}$ for almost all $t \in [0, \infty)$. We seek a condition on the controller gain k that ensures the global asymptotic stability of the unperturbed process (18), and yields the negative definite performance index (see [12] for more details)

$$\begin{aligned} \mathcal{J} &= \int_0^\infty [\|\phi(t, \cdot)\|_{L_2(0,1)}^2 - \gamma^2 \|h(t, \cdot)\|_{L_2(0,1)}^2] dt \\ &\quad - \gamma^2 \|\phi(0, \cdot)\|_{L_2(0,1)}^2 < 0 \end{aligned} \quad (35)$$

on the solutions of the perturbed system (34) for any $h \in L_2(0, \infty; \mathbf{W})$ and some constant γ . For solving the problem we follow an idea, proposed in [13], and carry

out conditions that guarantee the negative definiteness of the form

$$\begin{aligned} \mathcal{W}(\phi(t, \cdot), h(t, \cdot)) &:= \eta_1 \gamma^2 \frac{dV(\phi(t, \cdot))}{dt} \\ &\quad + \|\phi(t, \cdot)\|_{L_2(0,1)}^2 - \gamma^2 \|h(t, \cdot)\|_{L_2(0,1)}^2 < 0 \end{aligned} \quad (36)$$

computed on the solutions of the perturbed system (34) with $V(\phi(t, \cdot))$ given by (25). Once (36) is guaranteed, integrating $\mathcal{W}(\phi(t, \cdot), h(t, \cdot))$ in t from 0 to ∞ and taking into account that $\limsup_{t \rightarrow \infty} V(\phi(t, \cdot)) \geq 0$ result in (35). Indeed, (36) ensures that

$$\begin{aligned} & -\eta_1 \gamma^2 \int_0^1 \phi(0, x)^2 \frac{x}{\eta_{||}(0, x)} dx + \\ & \int_0^\infty [\|\phi(t, \cdot)\|_{L_2(0,1)}^2 - \gamma^2 \|h(t, \cdot)\|_{L_2(0,1)}^2] dt < 0 \end{aligned} \quad (37)$$

and due to (13), the negative definiteness of (35) follows. In order to ensure (36) let us set $\zeta(t, x) = (|\phi(t, x)|, |h(t, x)|)^T$ and compute the time derivative of (25) along the solutions of the perturbed system (34). Similar to (31), we obtain that

$$\begin{aligned} \mathcal{W} &\leq \left[1 - 2\frac{\eta_1}{\eta_2} \gamma^2 \left(\frac{\eta_1^2 e}{\mu_0 a^2 \eta_2} + k - \frac{\Delta}{2\eta_1} \right) \right] \int_0^1 \phi(t, x)^2 x dx \\ &\quad + 2\gamma^2 \int_0^1 |h(t, x)| |\phi(t, x)| x dx \\ &\quad - \gamma^2 \int_0^1 h(t, x)^2 x dx \leq \int_0^1 \zeta^T(t, x) \Phi_\gamma \zeta(t, x) x dx \end{aligned} \quad (38)$$

where

$$\Phi_\gamma := \begin{pmatrix} 1 - 2\frac{\eta_1}{\eta_2} \gamma^2 \left(\frac{\eta_1^2 e}{\mu_0 a^2 \eta_2} + k - \frac{\Delta}{2\eta_1} \right) & \gamma^2 \\ \gamma^2 & -\gamma^2 \end{pmatrix}. \quad (39)$$

If $\Phi_\gamma < 0$ then $\mathcal{W} < 0$. In turn, due to the Schur complements formula (see, e.g., [6, pp. 7-8] for details), the LMI $\Phi_\gamma < 0$ is satisfied if

$$1 - \frac{2\eta_1 \gamma^2}{\eta_2} \left(\frac{\eta_1^2 e}{\mu_0 a^2 \eta_2} + k - \frac{\Delta}{2\eta_1} \right) + \gamma^2 < 0.$$

Thus, the tuning rule

$$k > \frac{(1 + \gamma^2)\eta_2}{2\gamma^2\eta_1} - \frac{e\eta_1^2}{\mu_0 a^2 \eta_2} + \frac{\Delta}{2\eta_1}, \quad (40)$$

imposed on the parameter k , ensures the negative definiteness of Φ_γ . Summarizing, we arrive at the following.

Theorem 2 *Let the conditions of Theorem 1 be satisfied and let the tuning rule (40) be additionally imposed on the controller gain k . Then the uncertain system (34) is internally (under $h \equiv 0$) globally exponen-*

tially stable. Moreover, the admissible external disturbances $h \in L_2(0, \infty; \mathbf{W})$ are attenuated in the sense of (35).

Proof The first assertion is established by Theorem 1. Since relation (40) is in force it follows that (39) is negative definite and by means of (38) it results in (36). Then integrating (36) in t from zero to infinity and employing that V is positive definite yield (37) thereby concluding (35). The second assertion is thus established that completes the proof of Theorem 2. \square

4 Proportional integral state feedback synthesis

The main goal of this section is to design a controller that would completely reject time-invariant disturbances by using proportional integral feedback. For this purpose, we need to additionally assume that plasma resistivity is representable in the form

$$\eta_{||}(t, x) = f(t)g(x) \quad (41)$$

subject to the constraints

$$0 < f_1 \leq f(t) \leq f_2, \quad 0 < g_1 \leq g(x) \leq g_2 \quad (42)$$

with some constants f_1, f_2, g_1, g_2 . Such a realistic assumption is justified in [24,25,33]. Then, let us define the inner-product space

$$\mathbf{W}_g = \{ \Psi \in \mathbf{H}^2(0, 1) : \frac{\partial \Psi}{\partial x} \Big|_{x=0} = \Psi(1) = 0 \} \quad (43)$$

of differentiable functions equipped with the inner product space $\langle \Psi_1, \Psi_2 \rangle_{L_2(0,1)} = \int_0^1 \Psi_1(x)\Psi_2(x) \frac{x}{g(x)} dx$ and the induced norm $\|\Psi\|_{L_2(0,1)} = \sqrt{\int_0^1 |\Psi(x)|^2 \frac{x}{g(x)} dx}$. It is clear that the space \mathbf{W}_g is nothing else than the aforementioned space \mathbf{W} equipped with an equivalent norm.

4.1 Stabilization under time-invariant disturbances

Let us consider the following distributed (proportional integral feedback) control

$$\begin{aligned} \eta_{||}(t, x) R_0 j_{control}(t, x) &= -k\phi(t, x) \\ -k_1 \int_0^t \phi(s, x) ds &- \frac{\eta_{||}(t, x)}{\mu_0 a^2} \frac{1}{x} \frac{\partial}{\partial x} \left(x \frac{\partial \psi_r^{target}}{\partial x}(x) \right) \end{aligned} \quad (44)$$

where k and k_1 are weight parameters (to be defined) and $j_{control}$ is given by (11). Then the error state equation (16), driven by the proportional integral feedback (44) and additionally affected by a time-invariant external

disturbance $h(x) \in \mathbf{W}_g$, is specified to

$$\begin{cases} \frac{\partial \phi}{\partial t}(t, x) = \frac{\eta_{||}(t, x)}{\mu_0 a^2} \frac{1}{x} \frac{\partial}{\partial x} \left(x \frac{\partial \phi}{\partial x}(t, x) \right) - k\phi(t, x) \\ \quad - k_1 \int_0^t \phi(s, x) ds + h(x) \\ \frac{\partial \phi}{\partial x}(t, x) \Big|_{x=0} = 0, \quad \phi(t, 1) = 0. \end{cases} \quad (45)$$

In the subsequent analysis, the closed-loop system is shown to be globally asymptotically stable under an arbitrary $h(x) \in \mathbf{W}_g$.

Theorem 3 Let the controller gains are tuned according to

$$k > -\frac{f_1 g_1^2 e}{\mu_0 a^2 g_2}, \quad k_1 > 0. \quad (46)$$

Then the closed-loop system (45) is globally asymptotically stable in the state space \mathbf{W}_g regardless of whichever external disturbance $h(x) \in \mathbf{W}_g$ affects the system and hence $\phi_{steady\ state} = 0$.

Proof For later use, let us introduce an auxiliary variable $I(t, x)$ governed by

$$\frac{\partial I}{\partial t}(t, x) = \phi(t, x), \quad I(t = 0, x) = 0. \quad (47)$$

While being coupled to (47), system (45) under assumption (41) is augmented to

$$\begin{cases} \frac{\partial \phi}{\partial t}(t, x) = \frac{f(t)g(x)}{\mu_0 a^2} \frac{1}{x} \frac{\partial}{\partial x} \left(x \frac{\partial \phi}{\partial x}(t, x) \right) - k\phi(t, x) \\ \quad - k_1 I(t, x) + h(x) \\ \frac{\partial I}{\partial t}(t, x) = \phi(t, x) \\ \frac{\partial \phi}{\partial x}(t, x) \Big|_{x=0} = 0, \quad \phi(t, 1) = 0. \end{cases} \quad (48)$$

The steady state (ϕ_{ss}, I_{ss}) of system (48) is clearly defined by $\frac{\partial \phi_{ss}(t, x)}{\partial t} = 0, \quad \frac{\partial I_{ss}(t, x)}{\partial t} = 0$ that results in $\phi_{ss}(x) = 0, \quad I_{ss}(x) = \frac{h(x)}{k_1}$. On the solutions of (48), consider the functional

$$\begin{aligned} V(\phi(t, \cdot), I(t, \cdot)) &:= \frac{1}{2} \int_0^1 \phi(t, x)^2 \frac{x}{g(x)} dx \\ &\quad + \frac{k_1}{2} \int_0^1 \left(I(t, x) - \frac{h(x)}{k_1} \right)^2 \frac{x}{g(x)} dx \\ &:= V_1(t) + V_2(t) \end{aligned} \quad (49)$$

which proves to be positive definite and radially unbounded. Indeed,

$$V(\phi_{ss}, I_{ss}) = 0, \quad V(\phi, I) > 0 \quad \forall (\phi, I) \neq (\phi_{ss}, I_{ss}) \quad (50)$$

and $V(\phi, I) \rightarrow \infty$ as $\|\phi\|_{L_2(0,1)} + \|I\|_{L_2(0,1)} \rightarrow \infty$. Computing the time derivative

$$\begin{aligned} \frac{dV_1(t)}{dt} &= \frac{1}{2} \int_0^1 \frac{\partial}{\partial t} \left(\phi(t, x)^2 \frac{x}{g(x)} \right) dx \\ &= \int_0^1 \frac{\partial \phi(t, x)}{\partial t} \phi(t, x) \frac{x}{g(x)} dx \end{aligned} \quad (51)$$

of (49) on the solutions of (48) and employing the integration by parts yield

$$\begin{aligned}
\frac{dV_1(t)}{dt} &= \frac{f(t)}{\mu_0 a^2} \int_0^1 \frac{\partial}{\partial x} \left(x \frac{\partial \phi(t,x)}{\partial x} \right) \phi(t,x) dx \\
&\quad - k \int_0^1 \phi(t,x)^2 \frac{x}{g(x)} dx \\
&\quad - k_1 \int_0^1 I(t,x) \phi(t,x) \frac{x}{g(x)} dx \\
&\quad + \int_0^1 h(x) \phi(t,x) \frac{x}{g(x)} dx; \\
&= -\frac{f(t)}{\mu_0 a^2} \int_0^1 \left| \frac{\partial \phi(t,x)}{\partial x} \right|^2 x dx \\
&\quad - k \int_0^1 \phi(t,x)^2 \frac{x}{g(x)} dx - \frac{dV_2(t)}{dt}.
\end{aligned} \tag{52}$$

It follows that

$$\begin{aligned}
\frac{dV_1(t)}{dt} &= -\frac{f(t)}{\mu_0 a^2} \int_0^1 g(x) \left| \frac{\partial \phi(t,x)}{\partial x} \right|^2 \frac{x}{g(x)} dx \\
&\quad - k \int_0^1 \phi(t,x)^2 \frac{x}{g(x)} dx - \frac{dV_2(t)}{dt} \\
&< -\frac{f_1 g_1}{\mu_0 a^2} \int_0^1 \left| \frac{\partial \phi(t,x)}{\partial x} \right|^2 \frac{x}{g(x)} dx \\
&\quad - k \int_0^1 \phi(t,x)^2 \frac{x}{g(x)} dx - \frac{dV_2(t)}{dt}.
\end{aligned} \tag{53}$$

Taking into account that Lemma 1, being specified with $w(\cdot) = g(x)$ and $L(\cdot) = \phi(t, x)$, results in

$$\int_0^1 |\phi(t, x)|^2 \frac{x}{g(x)} dx \leq \frac{g_2 e^{-1}}{g_1} \int_0^1 \left| \frac{\partial \phi(t, x)}{\partial x} \right|^2 \frac{x}{g(x)} dx \tag{54}$$

one then arrives at

$$\begin{aligned}
\frac{dV(\phi(t, \cdot))}{dt} &= \frac{dV_1(t)}{dt} + \frac{dV_2(t)}{dt} \\
&< -\left(\frac{f_1 g_1^2 e}{\mu_0 a^2 g_2} + k \right) \int_0^1 \phi(t, x)^2 \frac{x}{g(x)} dx.
\end{aligned} \tag{55}$$

Due to (46), one concludes that $\frac{dV(\phi(t, \cdot))}{dt} \leq 0$ and

$$\frac{dV(\phi(t, \cdot))}{dt} = 0 \Rightarrow \int_0^1 \phi(t, x)^2 \frac{x}{g(x)} dx = 0 \tag{56}$$

i.e., $\phi(t, x) = 0 = \phi_{ss}$ once $\frac{dV(\phi(t, \cdot))}{dt} = 0$. Moreover, relation $\phi(t, x) = 0 = \phi_{ss}$, coupled to (47), ensures that $I(t, x) = \frac{h(x)}{k_1} = I_{ss}$, thereby concluding that the maximal invariant manifold of $\frac{dV(\phi(t, \cdot))}{dt} = 0$ coincides with $(\phi, I) = (\phi_{ss}, I_{ss})$. Thus, by applying the LaSalle invariance principle to the parabolic system (48) (see [15] for the invariance principle extension to parabolic systems), the desired global asymptotic stability is established. Hence, system (45) is globally asymptotically stable in \mathbf{W} under an arbitrary $h(x) \in \mathbf{W}_g$. \square

4.2 \mathcal{H}_∞ design

The objective of this subsection is to show that in addition to the rejection of time-invariant external disturbances, the proposed controller (44) attenuates time-varying disturbances with a certain level $\gamma > 0$. Let

us suppose that the disturbance h affecting system (45) varies in time, thus resulting in the state equation

$$\begin{cases} \frac{\partial \phi}{\partial t}(t, x) = \frac{f(t)g(x)}{\mu_0 a^2} \frac{1}{x} \frac{\partial}{\partial x} \left(x \frac{\partial \phi}{\partial x}(t, x) \right) - k\phi(t, x) \\ \quad - k_1 \int_0^t \phi(s, x) ds + h(t, x) \\ \frac{\partial \phi}{\partial x}(t, x) \Big|_{x=0} = 0, \quad \phi(t, 1) = 0 \end{cases} \tag{57}$$

where $h(t, \cdot) \in L_2(0, \infty; \mathbf{W}_g)$ is an external disturbance of cumulative finite energy. We seek an additional condition on the proportional integral controller gain k that would ensure the negative performance index

$$\begin{aligned} \mathcal{J}_g &= \int_0^\infty [\|\phi(t, \cdot)\|_{L_2(0,1)}^2 - \gamma^2 \|h(t, \cdot)\|_{L_2(0,1)}^2] dt \\ &\quad - \gamma^2 \|\phi(0, \cdot)\|_{L_2(0,1)}^2 < 0 \end{aligned} \tag{58}$$

on the solutions of (57) for all time-varying disturbances $h(t, \cdot) \in L_2(0, \infty; \mathbf{W}_g)$ with a constant attenuation level $\gamma > 0$. As before, $L_2(0, \infty; \mathbf{W}_g)$ stands for the Hilbert space of square integrable Hilbert space-valued functions $h(\cdot, x) \in L_2(0, \infty)$ with values $h(t, \cdot) \in \mathbf{W}_g$ for almost all $t \in [0, \infty)$. For establishing (58), it suffices to demonstrate that

$$\begin{aligned} \mathcal{W}_g(\phi(t, \cdot)) &:= 2\gamma^2 \frac{d}{dt} V_g(\phi(t, \cdot)) \\ &\quad + \int_0^1 (\phi(t, x)^2 - \gamma^2 h(t, x)^2) \frac{x}{g(x)} dx < 0 \end{aligned} \tag{59}$$

where

$$V_g(\phi(t, \cdot)) = \frac{1}{2} \int_0^1 \phi(t, x)^2 \frac{x}{g(x)} dx + \frac{k_1}{2} \int_0^1 I(t, x)^2 \frac{x}{g(x)} dx \tag{60}$$

Indeed, integrating $\mathcal{W}_g(\phi(t, \cdot))$ in t from 0 to ∞ and taking into account that $\limsup_{t \rightarrow \infty} V_g(\phi(\infty, \cdot)) \geq 0$ result in (58). Let us now compute the time derivative of functional (60) on the solutions of (57):

$$\begin{aligned} \frac{dV_g(\phi(t, \cdot))}{dt} &\leq -\left(\frac{f_1 g_1^2 e}{\mu_0 a^2 g_2} + k \right) \int_0^1 \phi(t, x)^2 \frac{x}{g(x)} dx \\ &\quad + \int_0^1 h(t, x) \phi(t, x) \frac{x}{g(x)} dx. \end{aligned} \tag{61}$$

Setting $\zeta = (|\phi(t, x)| \quad |h(t, x)|)^T$, it follows

$$\begin{aligned} \mathcal{W}_g &\leq \left(1 - 2\gamma^2 \left(\frac{f_1 g_1^2 e}{\mu_0 a^2 g_2} + k \right) \right) \int_0^1 \phi(t, x)^2 \frac{x}{g(x)} dx \\ &\quad + 2\gamma^2 \int_0^1 |h(t, x)| |\phi(t, x)| \frac{x}{g(x)} dx \\ &\quad - \gamma^2 \int_0^1 |h(t, x)|^2 \frac{x}{g(x)} dx \leq \int_0^1 \zeta^T \Psi_\gamma \zeta \frac{x}{g(x)} dx \end{aligned} \tag{62}$$

where

$$\Psi_\gamma := \begin{pmatrix} 1 - 2\gamma^2 \left(\frac{f_1 g_1^2 e}{\mu_0 a^2 g_2} + k \right) & \gamma^2 \\ \gamma^2 & -\gamma^2 \end{pmatrix}. \tag{63}$$

If $\Psi_\gamma < 0$ then $\mathcal{W}_g < 0$. By Schur's Lemma, the LMI condition $\Psi_\gamma < 0$ is satisfied if

$$k > -\frac{f_1 g_1^2 e}{\mu_0 a^2 g_2} + \frac{1}{2\gamma^2} + \gamma^2. \quad (64)$$

Hence, $\mathcal{W}_g < 0$ provided that k is chosen according to (64) and (58) is then guaranteed. Thus, the following result is in order.

Theorem 4 *Let the conditions of Theorem 3 be satisfied and let the tuning rule (64) be additionally imposed on the gain k of the proportional integral feedback (44). Then while being affected by a time-invariant external disturbance $h(x) \in \mathbf{W}_g$, the closed-loop system (57) is globally asymptotically stable in the state space \mathbf{W}_g . Moreover, all time-varying external disturbances $h(t, \cdot) \in L_2(0, \infty; \mathbf{W}_g)$ are attenuated in the sense of (58).*

Proof The first assertion is established by Theorem 3. By virtue of (64), matrix (63) is negative definite. Coupled to (62), this results in (59). Now to justify (58) it suffices to integrate (59) in t from zero to infinity and in the resulting inequality

$$\int_0^\infty [\|\phi(t, \cdot)\|_{L_2(0,1)}^2 - \gamma^2 \|h(t, \cdot)\|_{L_2(0,1)}^2] dt + 2\gamma^2 V_g(\phi(\infty)) - 2\gamma^2 V_g(\phi(0)) < 0, \quad (65)$$

to omit the positive definite term $2\gamma^2 V_g(\phi(\infty, \cdot))$ and to note that $2\gamma^2 V_g(\phi(0, \cdot)) = \gamma^2 \|\phi(0, \cdot)\|_{L_2(0,1)}^2$ due to (60), initialized in accordance with (47). Theorem 4 is thus proved. \square

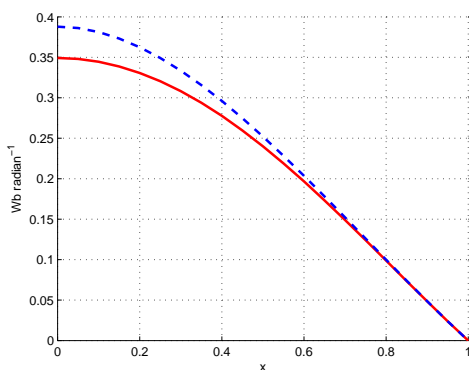


Fig. 3. Initial profile value $\psi_r(0, x)$ (dashed line) versus the target profile $\psi_r^{target}(x)$ (solid line)

5 Simulation results

We consider the relevant test where we want to control the evolution of the magnetic flux ψ_r from an initial profile to a target profile (see Fig. 3). To begin with,

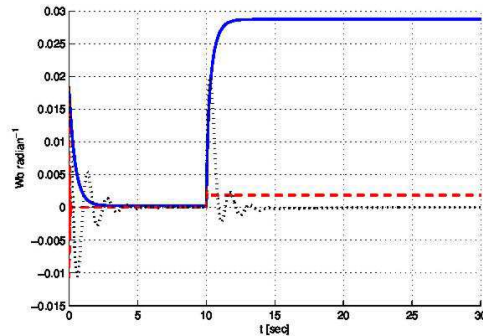


Fig. 4. Time evolution of ϕ profile at $x = 0.4$: solid line is for the gain values ($k = 1, k_1 = 0$), dashed line is for ($k = 80, k_1 = 0$), and dotted line is for ($k = 1, k_1 = 20$)

we performed a set of simulations on the infinite dimensional plant model, depicted in Fig. 2, to tune the proportional (k) and integral (k_1) gains. In these simulations, we did not use the engineering parameters optimization procedure, corresponding to the block "Model-based Optimization Algorithm" in Fig. 2. Instead, the \mathcal{H}_∞ controller $j_{control}$ was straightforwardly applied to the plant. We then also checked the effect of the disturbance

$$h(t, x) = \begin{cases} 0, & 0s \leq t < 10s \\ -\frac{1}{5\mu_0 R_0 a^2} \frac{1}{x} \frac{\partial}{\partial x} \left(x \frac{\partial \psi_r^{target}}{\partial x} \right), & 10s \leq t \leq 30s \end{cases} \quad (66)$$

added at the time instant $t = 10s$ and representing 20% of the target total current density $j_T^{target}(t, x)$, given by (3). The behavior of the closed loop system is illustrated by the time evolution of ϕ at point $x = 0.4$, given in Fig. 4 (a similar behavior was also obtained at other points x). As expected from theoretical results, obtained in section 3 and 4, (i) the closed loop system is asymptotically stable and the applied disturbance is additionally attenuated provided that the tuning rule of Theorem 1 and, respectively, that of Theorem 2 are satisfied; (ii) if confined to the proportional feedback only, the larger the proportional gain is applied the smaller the steady state error, resulting from a disturbance, is obtained; (iii) the time response can be speeded up by using a higher proportional gain but at the expense of possibly a higher overshoot; (iv) the integral gain allows one to cancel the steady state error resulting from the applied disturbance, higher values of the integral gain can speed up the attenuation of the applied disturbance at the expense of induced steady state oscillations.

In order to further validate the proposed control approach, the tokamak plant simulator METIS is used [2]. METIS is a simplified version of the CRONOS suite of codes [1] well suited to the final simulation test of tokamak control algorithms on physics relevant model, as simulating typical 20s long Tore Supra tokamak plasma

discharges takes typically 3 hours. The METIS code includes a full fast current diffusion solver and takes into account various nonlinear couplings between physical quantities. In the following, METIS was used jointly with the *Matlab/SimulinkTM* toolbox to simulate Tore Supra plasma discharges. Preliminary METIS open loop simulation based on real pulse engineering inputs ($V_0 = 0V$, $P_{lh} = 4.8MW$ and $N_{lh} = 1.7$) were performed in order to find a reachable target profile. The proportional integral feedback was then implemented using values of k and k_1 resulting from the previously mentioned tuning process where reasonably low values $k = 1s^{-1}$ and $k_1 = 0.8s^{-2}$ were chosen to avoid deal with high overshooting and induced steady state oscillations. At $t = 10.1s$, the controller was activated in order to force the magnetic flux profile to reach the target profile. The target profile was basically reached in $5.8s$. As in the preliminary infinite dimensional simulations, made without engineering parameter optimization, the disturbance $\tilde{h}(t, x) = h(t - 6, x)$, specified with (66), was added at $t = 16s$. Simulation results are presented in Figs. 5–8.

The time evolutions of the magnetic flux $\psi_r(t, x)$ versus the target profile $\psi_r^{target}(x)$ at the points $x = 0.2$, $x = 0.4$ and $x = 0.6$, and that of their integral discrepancy are shown in Fig. 5 and Fig. 6, respectively. Proportional integral feedback acts satisfactorily: a gentle dynamic behavior is observed and the stationary disturbance is properly attenuated on a sensible time scale. The time evolution of the engineering plant inputs is plotted in Fig. 7. The time evolutions of the relevant control deviation $\varepsilon_{rel}(t, x) = \frac{j_{control}(t, x) - j_{engineering}(t, x)}{j_{control}(t, x)}$ at the points $x = 0.1$ and $x = 0.5$ are shown in Fig. 8. It is concluded from Figs. 5–8 that due to the \mathcal{H}_∞ approach used, the essential discrepancy between $j_{engineering}(t, x)$ and $j_{control}(t, x)$ is properly attenuated along with the applied disturbance \tilde{h} , so that the target profile is approached in an appropriate time less than $6s$.

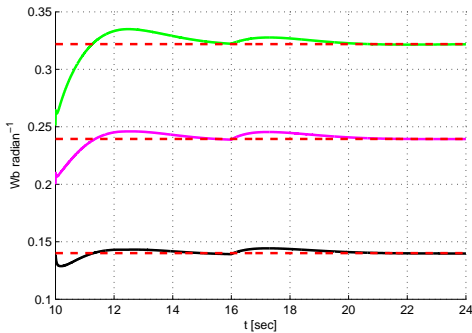


Fig. 5. Time evolution of ψ_r (solid line) versus the target ψ_r^{target} (dashed line) at $x = 0.2$ (the upper plot), at $x = 0.4$ (the middle plot), and at $x = 0.6$ (the lower plot)

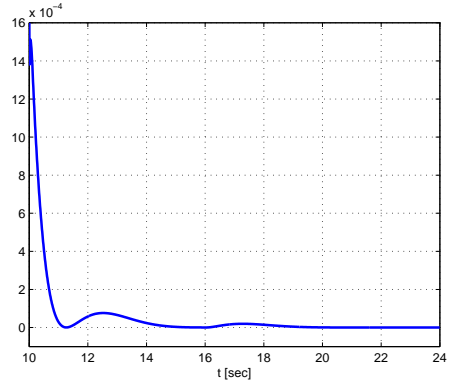


Fig. 6. Time evolution of $\int_0^1 [\psi_r(t, x) - \psi_r^{target}(x)]^2 dx$

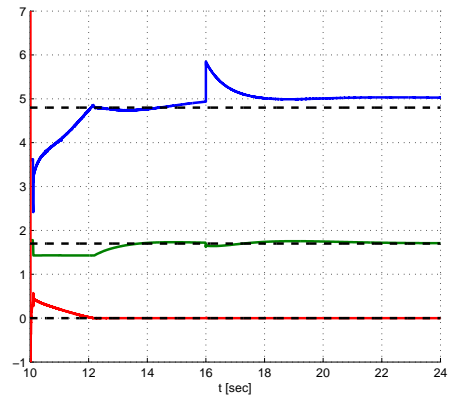


Fig. 7. Time evolution of the engineering inputs versus their nominal values, used for producing the target profile $\psi_r^{target}(x)$: the upper plot is for P_{LH} in megaWatt, the middle plot is for N_{LH} , the lower plot is for V_0 in Volt

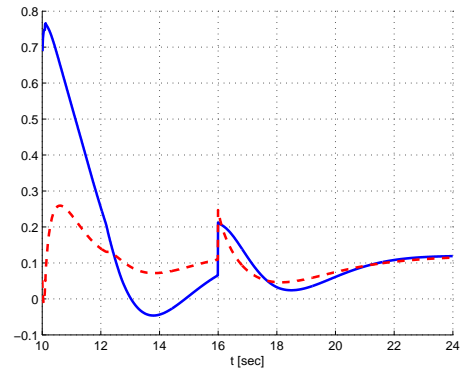


Fig. 8. Time evolutions of the relevant deviation $\varepsilon_{rel}(t, x) = \frac{j_{control}(t, x) - j_{engineering}(t, x)}{j_{control}(t, x)}$, computed at $x = 0.1$ (solid line), and that computed at $x = 0.5$ (dashed line)

6 Concluding remarks

In this paper, a \mathcal{H}_∞ control has been designed in the infinite dimensional setting for the tokamak plasmas cur-

rent profile using 1D resistive diffusion PDE of the magnetic flux. The investigated PDE system was reformulated so as to carry out a Lyapunov functional of the resulting system. Then an LMI based approach was applied to \mathcal{H}_∞ control design in infinite dimensional setting in order to propose two controllers (proportional state feedback for stabilization and disturbance attenuation and proportional integral controller for stabilization and attenuation of time-invariant disturbances). A model-based optimization procedure was used in the simulations to derive the engineering plant inputs related to both inductive and non-inductive current drive means. The numerical simulations were performed using typical Tore Supra values that yield quite positive results with promising robustness properties.

Acknowledgements

This work was partially supported by ANR-12-BS03-008-03 and by ITER (FRCM).

References

- [1] J. F. Artaud et al. The cronos suite of codes for integrated tokamak modeling. *Nuclear Fusion*, 50(4):1–25, 2010.
- [2] J.F. Artaud. Metis User’s Guide. Technical report, CEA, IRFM, January 2008.
- [3] O. Barana et al. Feedback control of the lower hybrid power deposition profile on Tore Supra. *Plasma Phys. Control. Fusion*, 49(7):947967, 2007.
- [4] A. Becoulet et al. Steady state long pulse tokamak operation using lower hybrid current drive. *Fusion Engineering and Design*, 86(6-8):490–496, 2011.
- [5] J. Blum. *Numerical Simulation and Optimal Control in Plasma Physics With Applications to Tokamaks*. Wiley / Gauthier-Villars Series in Modern Applied Mathematics, 1989.
- [6] S. Boyd et al. *Linear Matrix Inequalities in System and Control Theory*. Society for Industrial & Applied Mathematics, U.S., 1987.
- [7] F. Bribiesca-Argomedo et al. Model-based Control of the Magnetic Flux Profile in a Tokamak Plasma. In *Proceedings of the 49th IEEE Conference on Decision and Control*, Atlanta, GA, USA, 2010.
- [8] F. Bribiesca-Argomedo et al. Polytopic Control of the Magnetic Flux Profile in a Tokamak Plasma. In *Preprints of the 18th IFAC World Congress*, Milano (Italy) August 28 - September 2, 2011, 2011.
- [9] F. Bribiesca-Argomedo et al. A strict control lyapunov function for diffusion equation with time-varying distributed coefficients. *IEEE Transactions on Automatic Control*, DOI 10.1109/TAC2012.2209260.
- [10] C. D. Challis. The use of internal transport barriers in tokamak plasmas. *Plasma Physics and Controlled Fusion*, 46(12B):B23–B40, 2004.
- [11] J. M. Coron. *Control and Nonlinearity*. American Mathematical Society, 2007.
- [12] C. Du and L. Xie. *H_∞ Control and Filtering of Two-dimensional Systems*. Springer-Verlag Berlin and Heidelberg GmbH & Co. K, 2002.
- [13] E. Fridman and Y. Orlov. An LMI approach to H_∞ boundary control of semilinear parabolic and hyperbolic systems. *Automatica*, 45(9):2060–2066, 2009.
- [14] O. Gaye et al. Sliding mode stabilization of the current profile in tokamak plasmas. In *Proceedings of the 50th IEEE Conference on Decision and Control*, Orlando, Florida, USA, 2011.
- [15] D. Henry. *Geometric Theory of Semilinear Parabolic Equations*. Lecture Notes in Mathematics, Springer-Verlag, Berlin, 1981.
- [16] S.P. Hirshman. Finite-aspect-ratio effects on the bootstrap current in tokamaks. *Phys. Fluids*, 10(31):3150–3152, 1998.
- [17] F. Imbeaux et al. Real-time control of the safety factor profile diagnosed by magneto-hydrodynamic activity on the Tore Supra tokamak. *Nucl. Fusion*, 51(7):1–12, 2011.
- [18] V. Komornik and P. Loreti. *Fourier Series in Control Theory*. Springer-Verlag, 2005.
- [19] A. Kufner and L. E. Persson. *Weighted inequalities of Hardy type*. World Scientific Publishing Company, 2003.
- [20] D. Moreau et al. A two-scale dynamic model approach for magnetic and kinetic profile control in advanced tokamak scenarios on jet. *Nucl. Fusion*, 48(10):1–38, 2008.
- [21] D. Moreau et al. Plasma models for real-time control of advanced tokamak scenarios. *Nucl. Fusion*, 51(6):1–14, 2011.
- [22] P. Moreau et al. Plasma control in Tore Supra. *Fusion Science and Technology*, 56(3):1284–1299, 2009.
- [23] Y. Orlov. Discontinuous unit feedback control of uncertain infinite-dimensional systems. *IEEE transactions on automatic control*, 45(2):834–843, 2000.
- [24] Y. Ou et al. Optimal tracking control of current profile in tokamaks. *IEEE Transaction on Control Systems Technology*, 19(2):432–441, 2011.
- [25] Y. Ou et al. Receding-horizon optimal control of the current profile evolution during the ramp-up phase of a tokamak discharge. *Control Engineering Practice*, 19(1):22–31, 2011.
- [26] H. Ouarit et al. Validation of plasma current profile model predictive control in tokamaks via simulations. *Fusion Engineering and Design*, 86(6-8):1018–1021, 2011.
- [27] B. Saoutic et al. Tore supra : toward steady state in a superconducting tokamak. *Fusion Science and Technology*, 56(3):1079–1091, 2009.
- [28] A. Smyshlyaev and M. Krstic. *Adaptive Control of Parabolic PDEs*. Princeton University Press, 2010.
- [29] J. Wesson. *Tokamaks 3rd Edition by John Wesson*. Oxford University Press, 2004.
- [30] T. Wijnands et al. Feedback control of the current profile on Tore Supra. *Nucl. Fusion*, 37(6):777–791, 1997.
- [31] E. Witrant et al. A control-oriented model of the current profile in tokamak plasma. *Plasma Phys. Control. Fusion*, 49(7):1075–1105, 2007.
- [32] www.iter.org.
- [33] C. Xu et al. Sequential linear quadratic control of bilinear parabolic PDEs based on POD model reduction. *Automatica*, 47(2):418–426, 2011.